BILINGUAL PUBLISHING GROUP

Journal of Mechanical Materials and Mechanics Research
https://journals.bilpubgroup.com/index.php/jmmmr

ARTICLE

Offline Trajectory Generation for Bipedal Robot Using Linear Inverted Pendulum Model

Navneet Ratre, S.K. Panigrahi*, Shivam Dubey

Department of Mechanical Engineering, Defence Institute of Advanced Technology, Pune, Maharashtra, 411025, India

ABSTRACT

Reduced order model (ROM)-based controllers have proved to be effective to generate stable bipedal locomotion. However, it is important to understand the limitations and effectiveness of these models without implementing any controllers. This study highlights the versatility of the Linear Inverted Pendulum Model (LIPM) at various walking speeds. Firstly, the Centre of Mass (COM) trajectory has been generated using the LIPM model, and the foot motion trajectory has been created using a sixth-order polynomial function. The trajectory is generated using a predefined step length, speed of locomotion and COM height. Secondly, the task space trajectory has been converted into a joint space trajectory through inverse kinematics for a 6-degree-of-freedom leg. To facilitate the proper walking motion the contact between the foot sole and the ground is implemented. Finally, a simple bipedal robot in MATLAB/Simulink has been modelled and the generated trajectories were implemented.

Keywords: Bipeds; Gait; Inverse kinematics; Joint space; Reduced order model (LIPM); Task space; Trajectory

1. Introduction

The concept of robotics has emerged as a result of advancements in automata. In the 18th century, a mechanical doll known as "Karakuri ningyo" was created to serve tea and act as an archer. Later, in 1920, Karel Capek introduced the term "robot" in his play "Rossum's Universal Robots (RUR)". Industrial robots were developed as a consequence of these early advancements, enabling them to work with humans to perform repetitive tasks, such as painting, bolting, riveting, and pick-and-place operations. As technology advanced throughout the 20th century,

*CORRESPONDING AUTHOR:
S.K. Panigrahi, Department of Mechanical Engineering, Defence Institute of Advanced Technology, Pune, Maharashtra, 411025, India; Email: panigrahisk@diat.ac.in; panigrahi.sk@gmail.com

ARTICLE INFO
Received: 25 July 2023 | Revised: 15 August 2023 | Accepted: 25 August 2023 | Published Online: 28 August 2023
DOI: https://doi.org/10.30564/jmmmr.v6i2.5852

CITATION
Ratre, N., Panigrahi, S.K., Dubey, S., 2023. Offline Trajectory Generation for Bipedal Robot Using Linear Inverted Pendulum Model. Journal of Mechanical Materials and Mechanics Research. 6(2): 39-48. DOI: https://doi.org/10.30564/jmmmr.v6i2.5852

robots were integrated with machine learning and artificial intelligence, making them more advanced and sophisticated. Throughout history, humans have exploited the natural environment to further their own development. To adapt to the human world, robots have been developed to imitate human behaviour, leading to the creation of humanoids. Humans rely on their upper bodies for manipulation and observation tasks, while mobility is achieved through leg movement. Robotics has long been involved in object manipulation and handling, with early robot designs relying on wheel motion. The use of wheels offers several benefits, such as efficiency, ease of control, and fast execution. However, wheel robots have many limitations since they cannot reach all areas on Earth that legged animals can access. Consequently, there has been a shift towards legged robots. The first legged robot, the planar hopping machine, was capable of traveling at a speed of approximately 0.8 m/s. Subsequent developments led to the creation of robots with prismatic legs, where the legs extend during the gait cycle. The prismatic leg mechanisms have been used in both two-legged robots that mimic human motion and four-legged robots that move like dogs. Humans learn to walk at a very early age, taking about a year or two to achieve a balanced gait. This illustrates that even when we are standing, our joints are in an active state. Similarly, humanoids maintain balance on their foot support, but due to the small support area, they are highly unstable. Even the slightest disturbance can cause the robot to fall.

We learn from childhood that the human body has 206 bones connected by 360 joints. The most advanced robots to date have yet to match the complexity of the human body structure. In 2016, the University of Tokyo created a humanoid named Kengoro, which has 174 degrees of freedom (DOF), the highest of any humanoid to date. Other humanoids, such as Atlas and Optimus, have 28 joints, while NASA's Robonaut 2 has approximately 42 DOF. The humanoid's configuration is typically decoupled into two parts: the upper part for manipulation and the lower part, called the Biped, for movement in the 3D world.

The Biped consists of a torso and two legs with a common configuration. Each leg includes six joints: a spherical joint at the hip, a pitch joint at the knee, and a pitch-roll joint at the ankle. According to Piper et al. [1], if a 6 DOF robot manipulator has a spherical joint, its kinematics can be decoupled into two parts. The first part determines the position of the end effector, while the second part provides its orientation. Some researchers have also developed iterative algorithms that use Jacobeans. However, according to De Angulo et al. [2] the Jacobian method is velocity-based and does not consider the position of the end-effector, leading to significant accumulation of error in position.

Vukobratovic and Borovac's [3] research presented a fundamental idea for the development of bipedal dynamic locomotion, stating that the centre of pressure must remain within the support polygon to maintain balance while walking on a flat surface. This concept has become a widely accepted approach to ensuring stability in bipedal robots. As a result, numerous studies have been conducted on the development of controllers based on the Zero Moment Point (ZMP) concept.

Choi, Youngjin et al. [4] proposed a method to generate the actual trajectory for stable bipedal locomotion using a desired COM/ZMP trajectory. They modified the ZMP trajectory and evaluated the response. They also presented a new kinematic resolution method that incorporated stability during the motion of other body parts, such as moving the arms while walking. The authors demonstrated the robustness of this method and showed promising results for whole-body coordination. Kajita et al. [5] made significant contributions to the development of stable locomotion for bipedal robots. They used the concept of the Linear Inverted Pendulum Model (LIPM) to generate trajectories for the robot's center of mass (COM) and Zero Moment Point (ZMP). They also introduced the concept of "primitives", which are pre-defined motions that can be combined to generate more complex behaviors. With these techniques, they were able to develop controllers for the stable locomotion of a 12 DOF bipedal robot, which was able to walk on uneven terrain and even climb stairs.

Bipeds are capable of both static and dynamic locomotion. Static locomotion involves slow movement, but provides better stability, while dynamic locomotion is faster but less stable. The study of dynamic locomotion is a broad field with researchers generating trajectories for all joints and dynamics, as well as developing simplified models called Reduced Order Models (ROMs) for reliable results. These task-specific ROMs vary for different scenarios, such as the LIPM model for walking and the SLIPM model for running. The objectives of the present research are:

·Trajectory generation for the COM using the LIPM model for different locomotion speeds,

·Generation of foot trajectory for foot elevation and,

·Conversion of task space trajectory to Joint space trajectory using Inverse Kinematics Simulation of the biped in MATLAB/Simulink.

The proceeding section will provide the methods developed for trajectory generation. The subsequent sections will give the desired trajectory for the classical LIPM model, provides the contact modelling between foot and base, joint trajectories which are generated by using the IK and provides the Simulink model and simulation results of the work presented.

2. Dynamic modelling of bipedal robot

2.1 Dynamic locomotion

The dynamic motions are identified as the true animal-like walking motion. Much research has taken place to capture the gait mechanisms of animals and humans. In the case of dynamic locomotion, contrary to static locomotion, the COM could lie outside the support polygon. Here a new model proposed by Vukobratovich et al. [3] appears the zero moment (ZMP) point is the point of the pressure of the whole body. The ZMP should not cross the support polygon for dynamically stable locomotion. If the ZMP leaves the support polygon, the biped requires more power to recover the unbalance motion. In this case, the location of the ZMP of a planned biped trajectory affects the balance during the dynamic motion.

2.2 Gait

The gait of any robot defines the manner of walking or moving on the foot. In simple words, we can say that it is the walking pattern of the robot, which it follows, and have stable motion. It is assumed that the biped Gait is similar to the 3D Pendulum [6]. The Gait consists of the information on the foot placement, the position of the center of mass (COM) the velocity of the locomotion, and the location of the ZMP for each instance of time. In addition, it gives information about the different phases of the locomotion, (the single support phase and the double support phase). It also determines the information on the time of the support exchange. The Gait for the robot can be modeled by taking the dynamic equation or without it. It generally forms the framework of the motion of the leg-foot placement. By setting a proper constraint plane, a pattern can be generated to walk on the stairs and some uneven terrains. While in motion, the biped sometimes has its one-foot on the ground, and sometimes both feet on the ground. These conditions are categorized into two: SSP (single support phase) and DSP (double support phase). Both phases occur sequentially. Majority of the time the biped is in SSP condition.

2.3 LIPM

Linear Inverted Pendulum Model (LIPM) model as shown in **Figure 1** is the 'task based motion constrained' form of the inverted pendulum model (IPM). The LIPM consists of a point mass at the end of a massless leg having variable length. As the model is composed of angular motion, it is beneficial to use the polar coordinates to generate the equation of motion [7].

It is assumed that the vertical motion of the COM is negligible so the vertical acceleration can be omitted from the equation of motion. To impose the vertical motion, $z_g = const$, we need to model the equation of motion in Cartesian coordinates:

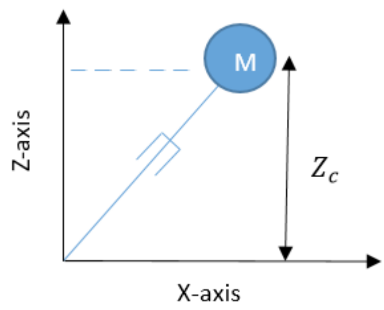

Figure 1. Linear inverted pendulum model.

$$M\ddot{x}_g = f_s \sin\theta \tag{1}$$

$$M(\ddot{z}_g + g) = f_s \cos\theta \tag{2}$$

Putting $z_g = const$,

$$M\ddot{x}_g = f_s \sin\theta \tag{3}$$

$$Mg = f_s \cos\theta \tag{4}$$

$$\ddot{x}_g = \omega_{LIP}{}^2(x_g - p_x) \tag{5}$$

$$\ddot{y}_g = \omega_{LIP}{}^2(x_g - p_y) \tag{6}$$

where, x_g = Position of mass in the x-axis (x-axis is supposed to be the axis of frontal motion of biped);

y_g = Position of mass in the y-axis (y-axis is supposed to be the axis of sagittal motion of biped);

z_g = Position of mass in the Z-axis (Z-axis is supposed to be the axis of transverse motion of biped);

p_x = Center of pressure (COP) along x-axis;

p_y = Center of pressure (COP) along y-axis;

ω_{LIP} = Natural angular frequency of the pendulum.

$$\omega_{LIP} = \sqrt{\frac{g}{z_g}} \tag{7}$$

The closed form solution of the above nonlinear equation is given as:

$$x_g(t) = x_{g0}\cosh(\omega_{ZMP}t) + \frac{v_{xg0}}{\omega_{ZMP}}\sinh(\omega_{ZMP}t) \tag{8}$$

$$y_g(t) = y_{g0}\cosh(\omega_{ZMP}t) + \frac{v_{yg0}}{\omega_{ZMP}}\sinh(\omega_{ZMP}t) \tag{9}$$

3. Trajectory generation

3.1 Trajectory for COM using LIPM

Walking primitives

Referring to **Figure 2**, walking primitives consist of data predefined to generate the reference trajectories. It contains the position of the footsteps for each leg in lateral and frontal directions, the step length, number of steps for each foot.

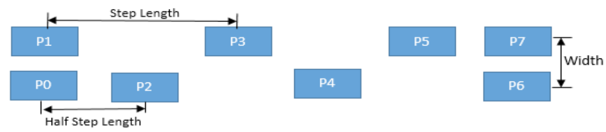

Figure 2. Walking primitives for the foot step.

The trajectory is generated in two phases:

·Trajectory for the torso (in lateral and frontal direction);

·Trajectory for the foot (in the transverse direction).

The solution to the above equation is as follows:

$$x_g = (x_{g0} - p_x)\cosh(\omega_{ZMP}t) + \frac{v_{xg0}}{\omega_{ZMP}}\sinh(\omega_{ZMP}t) \tag{10}$$

for $0 < t < T$

$$y_g = (y_{g0} - p_y)\cosh(\omega_{ZMP}t) + \frac{v_{yg0}}{\omega_{ZMP}}\sinh(\omega_{ZMP}t) \tag{11}$$

for $0 < t < T$

As mentioned above that the pressure points are constant and at the support leg during the single support phase. These pressure points are the required ZMP points at the foot sole [8].

$$p_x = x_g - \frac{1}{\omega_{ZMP}^2}\ddot{x}_g \tag{12}$$

$$p_y = y_g - \frac{1}{\omega_{ZMP}^2}\ddot{y}_g \tag{13}$$

Initially, we need to give a small trajectory so that it will start to move. The trajectory for the first step is generated by using fifth order polynomial to have the proper initial and final conditions of COM.

Trajectory for the first step

$y_{g0} = 0$

x_{ge} = half step length

$v_{xg0} = 0$

$v_{xge} = v_{end}$

$a_{xg0} = a_{end_2}$ (providing initial acceleration as the acceleration of mass at the end of second step)

$a_{xge} = a_{end_2}$ (initial acceleration and final acceleration are same for the trajectory along the direction of motion)

$$x_g = a_{x_0} + a_{x_1}t + a_{x_2}t^2 + a_{x_3}t^3 + a_{x_4}t^4 + a_{x_5}t^5 \quad (14)$$

$$v_{xg} = a_{x_1} + 2a_{x_2}t^1 + 3a_{x_3}t^2 + 4a_{x_4}t^3 + 5a_{x_5}t^4 \quad (15)$$

$$a_{xg} = 2a_{x_2} + 6a_{x_3}t^1 + 12a_{x_4}t^2 + 20a_{x_5}t^3 \quad (16)$$

The trajectory from the second step to n step

$$x_g = (x_{g0} - p_x)\cosh(\omega_{LIP}t) + \frac{v_{xg0}}{\omega_{LIP}}\sinh(\omega_{LIP}t) \quad (17)$$

for T < t < T+Ts

$$y_g = (y_{g0} - p_y)\cosh(\omega_{LIP}t) + \frac{v_{yg0}}{\omega_{LIP}}\sinh(\omega_{LIP}t) \quad (18)$$

for T < t < T+Ts

3.2 Trajectory for the foot elevation for the swing phase

To formulate the proper dynamical stable locomotion the trajectory should be composed of DSP and SSP, so that there should not be any disruption in the motion, this also ensures the jerk free motion of the biped. In many articles, it is mentioned that the DSP should be 20% and the SSP should be 80% of the total time taken for the step (Ts). For this, we have divided the DSP time period into two halves and put at the start and at the end of the trajectory.

Time for DSP = 0.2 Ts

Time for SSP = 0.8 Ts

Polynomial trajectory

The trajectory is generated by using sixth order polynomial as shown in **Figure 3** as the swing height is needed to be added along with the initial and final condition of the foot.

$$z_{Swing\ Foot} = \begin{Bmatrix} 0 & for\ 0 < t \le DSP/2 \\ z_g & for\ DSP/2 < t \le DSP/2 + SSP \\ 0 & for\ DSP/2 + SSP < t \le Ts \end{Bmatrix} \quad (19)$$

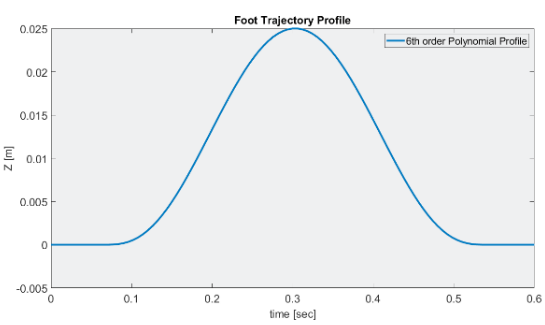

Figure 3. The trajectory for the foot elevation using sixth order polynomial function.

Initial conditions

$z_{g0} = 0$

$z_{g1} =$ Swing Height

$z_{g_{end}} = 0$

$\dot{z}_{g0} = 0$

$\dot{z}_{g_{end}} = 0$

$\ddot{z}_{g0} = 0$

$\ddot{z}_{g_{end}} = 0$

Equation for the profile:

$$z_g = a_{x_0} + a_{x_1}t + a_{x_2}t^2 + a_{x_3}t^3 + a_{x_4}t^4 + a_{x_5}t^5 + a_{x_6}t^6 \quad (20)$$

for DSP/2 < t < DSP/2 + SSP

$$\dot{z}_g = a_{x_1} + 2a_{x_2}t^1 + 3a_{x_3}t^2 + 4a_{x_4}t^3 + 5a_{x_5}t^4 + 6a_{x_6}t^5 \quad (21)$$

for DSP/2 < t < DSP/2 + SSP

$$\ddot{z}_g = 2a_{x_2} + 6a_{x_3}t^1 + 12a_{x_4}t^2 + 20a_{x_5}t^3 + 30a_{x_6}t^4 \quad (22)$$

for DSP/2 < t < DSP/2 + SSP

Both the legs have the same foot trajectory profile, just the other leg has a delay in motion by Ts period.

3.3 Leg motion repetition sequence

The left and the right legs work in the synchronized manor, also the trajectory repeats after every cycle. The simple algorithm behind the repetition of the gait can be understood by the following flow chart given in **Figure 4**:

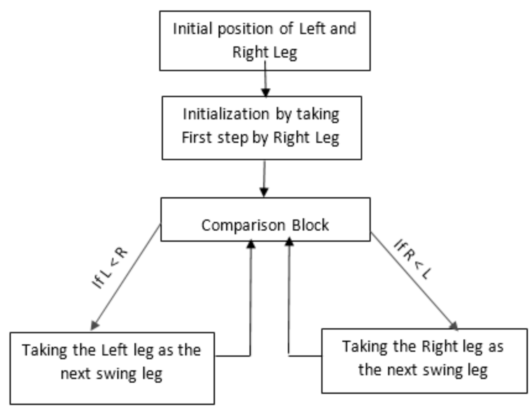

Figure 4. Repetition of gait sequence algorithm.

4. Contact modeling

As the humanoid robot moves, accurate information about the contact forces is crucial for maintaining stability. The contact model takes into account the virtual contact points to determine the position of the actual Center of Pressure (COP), called Zero Moment Point (ZMP), which validates the stability of the bipedal robot [3,9]. This information helps in ensuring that the bipedal robot maintains its stability during locomotion [10].

In our model, it is assumed that the biped is in contact with floor by its foot only. For these several virtual contact points are assigned at the sole of the foot. The contact can be modeled by using a simple spring damper mechanism in 3D which will act as friction cone. The Normal forces can be formulated by the following formulation:

$$f_{k_{nz}} = \begin{cases} -K_z \Delta z_n - D_z \Delta \dot{z}_n & (z_n < 0) \\ 0 & (z_n \geq 0) \end{cases} \tag{23}$$

$$f_{k_t} = \begin{cases} k_t \Delta t_n - D_t \dot{t}_n & \left(z_n < 0, \quad \sqrt{f_{k_{nx}}^2 + f_{k_{ny}}^2} \leq \mu_k f_{k_{nz}}\right. \\ \mu_k f_{k_{nz}} \dfrac{v_{k_{nt}}}{\sqrt{v_{k_{nx}}^2 + v_{k_{ny}}^2}} & \left(z_n < 0, \quad \sqrt{f_{k_{nx}}^2 + f_{k_{ny}}^2} > \mu_k f_{k_{nz}}\right. \\ 0 & (z_n \geq 0) \end{cases} \tag{24}$$

5. Inverse Kinematics for Joint Trajectories

The Transformation Matrix for the Distal Type DH parameter using the values of DH configuration for the leg as mentioned in **Table 1** [11,12] is given as:

$$T_i^{i-1} = \begin{pmatrix} cos(\theta_i) & -sin(\theta_i)\cos(\alpha_i) & sin(\theta_i)\sin(\alpha_i) & a_i cos(\theta_i) \\ sin(\theta_i) & cos(\theta_i)\cos(\alpha_i) & -cos(\theta_i)\sin(\alpha_i) & a_i sin(\theta_i) \\ 0 & \sin(\alpha_i) & \cos(\alpha_i) & d_i \\ 0 & 0 & 0 & 1 \end{pmatrix}$$

Table 1. D-H configuration for the leg.

DH (Distal) configuration for the leg				
Joint (i)	a_i	α_i	d_i	θ_i
1	0	90°	0	0
2	0	–90°	0	–90°
3	L_{Thigh}	0	0	0
4	L_{Tibia}	0	0	0
5	0	90°	0	0
6	L_{Foot}	0	0	0

As instructed by Ali et al. [13], we get to know that there are three joints intersecting at the torso, so the calculation needs to be done in the reverse order, so the torso becomes the end effector and the foot will act as a base. Now the joints responsible for the positioning of the end effector are θ_4, θ_5, θ_6.

$$C_4 = \frac{(p'_x + L_5)^2 + {p'_y}^2 + {p'_z}^2 - L_3^2 - L_4^2}{2L_3L_4} \tag{25}$$

$$\theta_4 = atan2(\sqrt{1 - C_4^2}, C_4) \tag{26}$$

$$\theta_5 = atan2\left(-p'_z, \pm\sqrt{(p'_x + L_5)^2 + {p'_y}^2}\right) - \mu \tag{27}$$

$$\mu = atan2(S_4L_3, C_4L_3 + L_4) \tag{28}$$

$$\theta_6 = atan2(p'_y, -p'_x - L_5) \tag{29}$$

Now as the location of the end effector is known, we can find the orientation by the remaining joint values θ_1, θ_2, θ_3.

$$\theta_2 = atan2\left(-\sqrt{1 - (S_6a'_x + C_6a'_y)^2}, S_6a'_x + C_6a'_y\right) + \frac{\pi}{2} \tag{30}$$

$$\theta_1 = atan2\left(-S_6s'_x - C_6s'_y, -S_6n'_x - C_6n'_y\right) + \pi \tag{31}$$

$$\theta_{345} = atan2(a'_z, C_6a'_x - S_6a'_y) \tag{32}$$

$$\theta_3 = \theta_{345} - \theta_4 - \theta_5 - \pi \tag{33}$$

6. Simulation model

6.1 Assumptions

In our model, the following assumptions were made before deploying for the simulation:

·The COM of the model will be at the same height throughout the motion.

·The foot will always be parallel to the plane of the ground even during the strike to the ground.

·The ZMP will always lie at the primitive points.

·The joints are frictionless.

·The COM of each link is at its center.

·The ground is modeled by the spring and damper system.

6.2 Model configuration

The model used for this simulation is generated in Simulink as shown in **Figure 5**. The model is a simplified bipedal robot which compose of center of mass at the center of each link and also have inertial properties. The model is composed of all revolute joints, where 3 joints (Yaw, Roll, and Pitch) at the junction of torso and leg, at the knee joint there is a Pitch joint and the ankle joint is composed of 2 joints (Pitch and Roll). The modal properties of links with respect to torso, thigh, tibia and foot are given in **Table 2**.

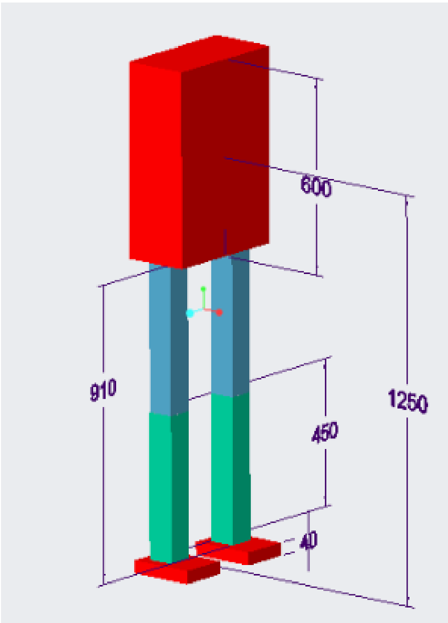

Figure 5. Simulink model for the simulation.

Position of a right leg with respect to torso center:

$$T(R) = \begin{bmatrix} -1 & 0 & 0 & 0.14 \\ 0 & -1 & 0 & 0 \\ 0 & 0 & 1 & -0.3 \\ 0 & 0 & 0 & 1 \end{bmatrix}$$

Position of Left leg with respect to torso center:

$$T(L) = \begin{bmatrix} -1 & 0 & 0 & -0.14 \\ 0 & -1 & 0 & 0 \\ 0 & 0 & 1 & -0.3 \\ 0 & 0 & 0 & 1 \end{bmatrix}$$

6.3 Modelling of virtual contact points at the foot sole

The model is composed of total of eight virtual contact points at the edges of each foot. **Figure 6** below shows the location of all the contact points of one foot:

Table 2. Modal properties.

Link	Dimension (m)	Mass (kg)	Inertia (kg.m^2)
Torso	[0.4, 0.2, 0.6]	48	[1.6, 2.08, 0.8]
Thigh	[0.46, 0.08, 0.08]	2.944	[0.00314027, 0.0534827, 0.0534827]
Tibia	[0.45, 0.08, 0.08]	2.88	[0.003072, 0.050136, 0.050136]
Foot	[0.04, 0.15, 0.2]	1.2	[0.00625, 0.00416, 0.00241]

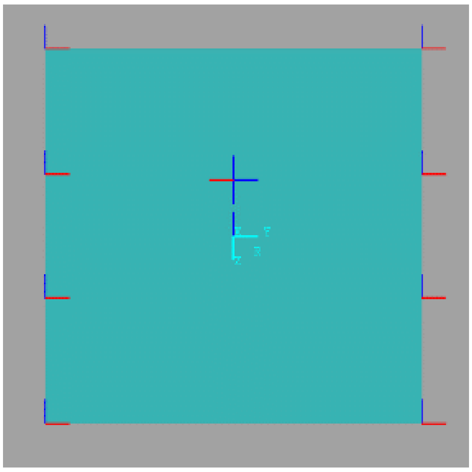

Figure 6. Eight virtual contact points at the foot sole.

7. Simulation results

The simulation of bipedal was carried out in the SIMULINK, and the trajectory was generated using the MATLAB script is shown in **Figure 7**. The Model used the 6-DOF joint to successfully move in the 3D world.

The trajectory generated using the reduced order model proposed was tested on the multilink humanoid robot. The foot contact model was implemented to have proper reaction and friction forces to make the robot move in the virtual world. The sequential repeated cycle of the leg locomotion for both legs was generated by the gait cycle function. It was assumed that the foot was always parallel to the ground throughout the motion. All the links in the Biped were assumed to have the same material properties.

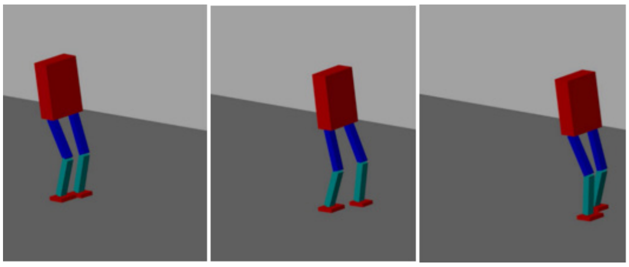

Figure 7. Simulated result of the walking robot in Simulink.

As the Bipedal moves in the direction of motion the COM have both lateral and frontal motion for dynamic stability. **Figure 8** shows the variation of the COM trajectory as the velocity of the locomotion varies also the vertices of the ZMP curve show the position of the foot placement. Foot trajectory profiles as shown in **Figure 9** for both legs are the same but have a delay of step period.

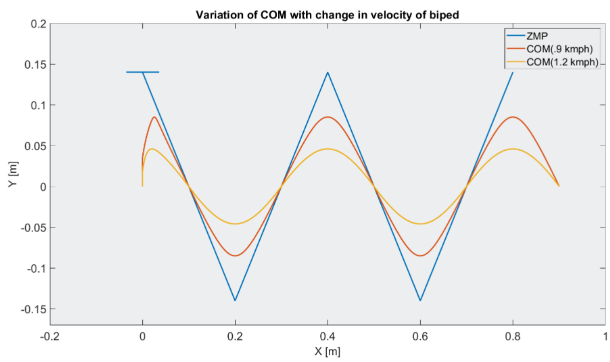

Figure 8. Variation of the COM trajectory with varying locomotion speed.

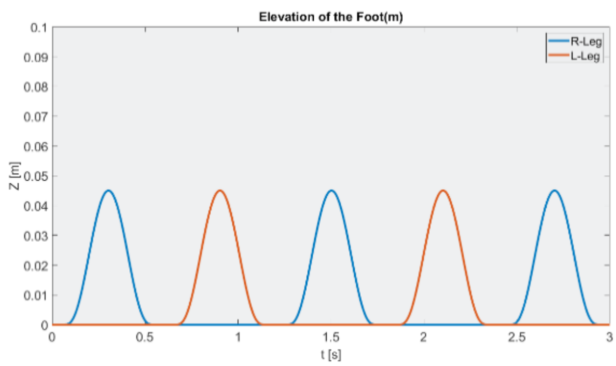

Figure 9. Foot elevation trajectory for both legs.

The desired trajectories for the ZMP and COM are generated using the LIPM model as discussed earlier in section 3. **Figure 10** shows the variation along the lateral as well as frontal direction of motion for both ZMP and COM.

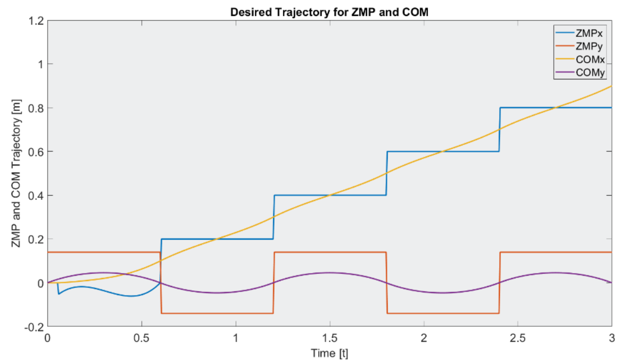

Figure 10. COM and ZMP trajectories in both axis with respect to time.

In the previous section, the trajectories for COM and foot were generated separately. The trajectory for the foot was generated considering the foot as the end effector and the torso as the base, but in the case of COM trajectory, the torso acts as the end effector, and the foot was the base frame. To have a single trajectory for both COM and foot, a new foot trajectory is generated for the motion in the lateral direction. This trajectory will give the same result but in the opposite direction. The resultant trajectory for both the foot from the given COM trajectory is shown in **Figure 11**.

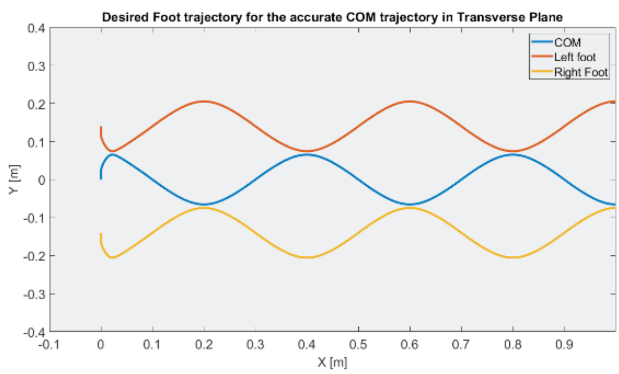

Figure 11. COM trajectory and the equivalent foot trajectories.

The reduced order models give the desired position and the desired orientation of the end effector in the task space. The trajectories are then converted into joint space trajectories as the robot takes the angular values for all the joints. In the Simulink model, we assumed that the joints are frictionless and the biped was able to move by joint values generated by IK exactly. **Figures 12-13** below shows the trajectories of each joint for the left and right leg respectively.

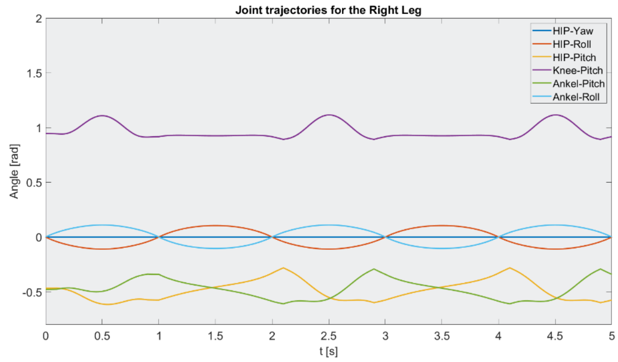

Figure 12. Joint trajectories for the right leg.

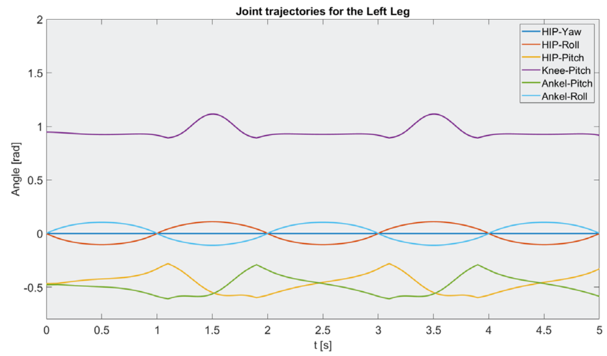

Figure 13. Joint trajectories for the left leg.

The Simulink model is provided with the Desired ZMP trajectory. **Figures 14-15** show the resultant of the actual trajectory followed by the bipedal robot for the locomotion at the speed of 0.9 kmph and 1.2 kmph respectively.

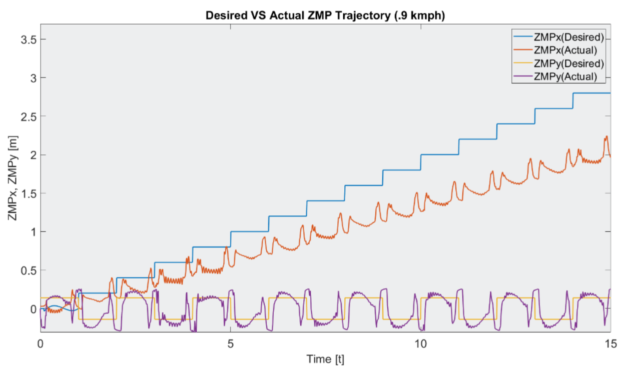

Figure 14. Actual and Desired ZMP trajectory at the speed of 0.9 kmph.

7.1 Outcomes

The simulation shows that the trajectory generated by the reduced order model is stable for dynamic locomotion. The LIPM was able to generate trajectories for a maximum step length 0.4 m with a walking speed of 1.2 kmph.

The biped becomes unstable at higher speeds and at low speeds (0.9 kmph).

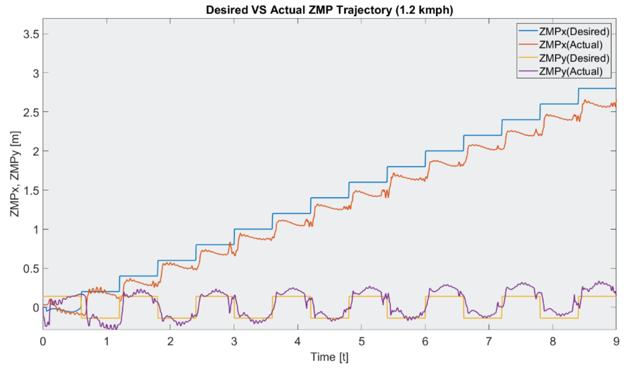

Figure 15. Actual and Desired ZMP trajectory at the speed of 1.2 kmph.

8. Conclusions

The foot trajectory formulated in this model would not be effective for too slow motion (static motion) as the trajectory for the foot and COM was generated simultaneously. To reduce the speed of motion to static motion, it would fall because the COM will no longer be at the support polygon, and for the static motion, the COM must be in the support polygon throughout the motion.

The trajectory of the foot plays a great role in the stability of the locomotion. In the present biped model, the trajectories were generated by using the sixth-order polynomial function. The function provides zero velocity at the time of contact of the foot with the ground. The actual ZMP of the simulation robot closely followed the desired trajectory, and the implementation of the controller will further improve the motion of the biped motion.

9. Future scope

The model could be tested for other Reduced Order Models listed above. It needs to ensure that the solution provided by these models is approximate, therefore it needs to be coupled with controllers so that it won't lose its track. As we can see in the simulation results, the simple model was not able to walk perfectly, this is because of ground reaction forces and the coupling forces due to the dynamic motion of the links. The actual robot composes of much more components like motors, batteries, system integrators, wires, and sensors etc., for this, the design of controllers is required.

Conflict of Interest

No potential conflict of interest was reported by the author(s).

References

[1] Pieper, D.L., 1969. The kinematics of manipulators under computer control. Stanford University: Stanford.

[2] Kajita, S., Morisawa, M., Miura, K., et al. (editors), 2010. Biped walking stabilization based on linear inverted pendulum tracking. 2010 IEEE/RSJ International Conference on Intelligent Robots and Systems; 2010 Oct 18-22; Taipei, Taiwan. New York: IEEE. p. 4489-4496.

[3] Vukobratović, M., Borovac, B., 2004. Zero-moment point—thirty five years of its life. International Journal of Humanoid Robotics. 1(1), 157-173.

[4] Choi, Y., Kim, D., Oh, Y., et al., 2007. Posture/walking control for humanoid robot based on kinematic resolution of com jacobian with embedded motion. IEEE Transactions on Robotics. 23(6), 1285-1293.

[5] Kajita, S., Kanehiro, F., Kaneko, K., et al. (editors), 2001. The 3D linear inverted pendulum mode: A simple modeling for a biped walking pattern generation. Proceedings 2001 IEEE/RSJ International Conference on Intelligent Robots and Systems. Expanding the Societal Role of Robotics in the the Next Millennium (Cat. No.01CH37180); 2001 Oct 29-Nov 3; Maui, HI, USA. New York: IEEE.

[6] Ohka, M., Yussof, H., 2010. Optimum biped trajectory planning for humanoid robot navigation in unseen environment. Robot Localization and Map Building. InTech: England. pp. 176-206.

[7] Wang, H., Tian, Y., Han, S., et al., 2017. ZMP theory-based gait planning and model-free trajectory tracking control of lower limb carrying exoskeleton system. Studies in Informatics and Control. 26(2), 161-170.

[8] Liu, Y., Zang, X., Heng, S., et al., 2017. Human-like walking with heel off and toe support for biped robot. Applied Sciences. 7(5), 499.

[9] Xhevahir, B., Ahmet, S., Gezim, H., et al., 2018. Dynamic modelling and analyzing of a walking of humanoid robot. Strojnícky časopis-Journal of Mechanical Engineering. 68(3), 59-76.

[10] Nenchev, D.N., Konno, A., Tsujita, T., 2018. Humanoid robots: Modeling and control. Butterworth-Heinemann: Oxford.

[11] Jazar, R.N., 2010. Theory of applied robotics. Springer Science + Business Media, LLC.: Berlin.

[12] Manipulator Dynamics [Internet]. Available from: https://ocw.snu.ac.kr/sites/default/files/NOTE/Chap06_Manipulator%20dynamics.pdf

[13] Ali, M.A., Park, H.A., Lee, C.G. (editors), 2010. Closed-form inverse kinematic joint solution for humanoid robots. 2010 IEEE/RSJ International Conference on Intelligent Robots and Systems; 2010 Oct 18-22; Taipei, Taiwan. New York: IEEE. p. 704-709.